Backstepping Control of Heavy Lift Operations with Crane Vessels

Ye, J.; Reppa, V.; Negenborn, R. R.

DOI
10.1016/j.ifacol.2020.12.1836

Publication date
2020

Document Version
Final published version

Published in
IFAC-PapersOnline

Available online at www.sciencedirect.com

ScienceDirect

IFAC Papers Online CONFERENCE PAPER ARCHIVE

IFAC PapersOnLine 53-2 (2020) 14704–14709

Backstepping Control of Heavy Lift Operations with Crane Vessels

J. Ye V. Reppa R.R. Negenborn *

* *Department of Maritime & Transport Technology, Delft University of Technology, 2628CD, the Netherlands (e-mail: {j.ye-1,v.reppa,r.r.negenborn}@tudelft.nl)*

Abstract: Offshore structures with large mass are installed and removed by heavy lift vessels. During offshore constructions, two safety-critical interconnected operations take place, the dynamic positioning of the vessel and the lifting of the heavy structure by an immovable boom crane on the vessel. Existing studies on offshore boom crane control either neglect the structure (load) dynamics in sway and the vessel movement, or consider the boom angle of the crane controllable. In this paper, we present a control scheme for underactuated offshore structure, taking into consideration the impact of the dynamic positioning of the vessel on the physical load model. The proposed control scheme is designed following a backstepping control approach using command filtering to generate virtual control signals and their derivatives avoiding the analytic differentiation. Simulation results are obtained by applying the control scheme in a dynamic positioned vessel-load model showing that the controller is able to stablize the load position during the vessel dynamic positioning.

Keywords: Backstepping control, Offshore heavy lift operation, Underactuated boom crane, Offshore installation, Command filtering.

1. INTRODUCTION

The economic growth worldwide has resulted in a significant increase of the demand of energy to fulfill the needs for people and industry. The exploration of energy resources has been extended from onshore to offshore, where huge platforms are installed to extract, store, and process oil and natural gas and windmills to produce wind energy (Sun et al., 2012). In order to reduce cost, stakeholders prefer to build such offshore structures onshore, then transfer and install them by heavy lift vessels offshore (Ye, 2016; Li et al., 2016). To perform the lifting of very heavy loads, huge cranes are located on the vessel. In addition to the installation of the offshore structures, the removal of such facility is also done by heavy lift vessels. According to the regulations of the International Maritime Organization (IMO), companies should remove the offshore installations when such facility is abandoned or disused in order to protect the environment (Hendrapati et al., 2017). For the stakeholders of such facility, it is also preferable to remove such offshore structures when the production is completed to save maintenance cost.

A heavy lift vessel is a vessel with a boom crane that has relatively high capacity (see Fig. 1), and should be distinguished from low capacity offshore cranes for containers. During the construction work, the angle of the boom crane stays constant or move in with very low angular velocity. The load (e.g. offshore structure) is connected to the crane winch via elastic metal wires. When the structure is free-hanging, it is affected by the environmental load and the motion of the vessel, which may lead to undesired swing and heave motion. Thus control systems were developed to stabilize the pay load during the time when it is hanging by the crane.

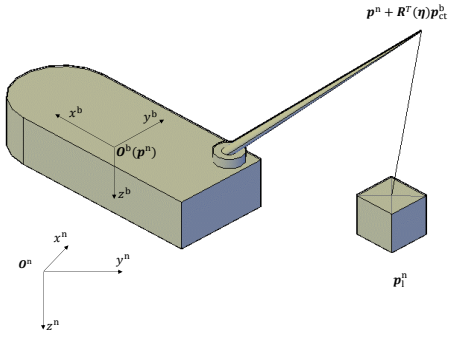

Fig. 1. Heavy Lift Vessel with Load, where $\boldsymbol{O}_{NED}$ is the orgin of earth-fixed coordinate system, $\boldsymbol{\eta}_3$ is the vessel position in the earth-fixed coordinate system and the origin of body-fixed coordinate system, $\boldsymbol{R}(\boldsymbol{\eta})$ is the transfer matrix from body-fixed coordinate system to earth-fixed coordinate system, $\boldsymbol{p}_{ct}$ is the body-fixed position of crane tip in the body-fixed coordinate system, $\boldsymbol{\eta}_l$ is the earth-fixed load position

Several researchers have proposed methods to improve the automatic control of offshore construction assignments. Previous research on this subject includes integration of dynamic positioning system (i.e. DP system, which is a

⋆ This work is financially supported by the program of China Scholarship Council (CSC) with project No. 20167720003.

10.1016/j.ifacol.2020.12.1836

computer-based system to control the horizontal motion of ship by means of thrusters and propellers) and crane vessel (Harmsen et al., 2018; Nam et al., 2013), nonlinear observer design (Ye et al., 2019b,a), and robust controller design (Ye et al., 2017). However, these studies only focus on the vessel DP system during construction, and do not consider the crane control.

For the control of offshore crane loads, existing methods can be classified as: i) active heave compensation of offshore load underwater (Messineo and Serrani, 2009) or above waterline (Küchler et al., 2010), where only heave position of the load is taken into consideration for control, ii) nonlinear control of offshore boom cranes for load position stabilization and trajectory tracking (Fang and Wang, 2012; Fang et al., 2013; Lu et al., 2017; Qian et al., 2017; Sun et al., 2017; Lu et al., 2019), where the center of gravity of the vessel is considered to be fixed with only roll movement, iii) adaptive controllers for fully actuated cranes with small capacity such as containers (Ismail and Ha, 2013; Chu et al., 2014; Nguyen et al., 2015; Ngo et al., 2019). Heavy lift vessels, however, is normally underactuated with very high lifting capacity, which is used for loads up to thousands of tonnes. The study of underactuated heavy load control under DP's impact is still missing in the literature.

The goal and the main contribution of this work is the design of a nonlinear control scheme for an underactuated crane-load model, considering the impact from the DP controlled vessel. In this paper,we design a controller for underactuated offshore heavy lift crane, taking into consideration the position and rotation of the vessel. The proposed controller is based on command filtered backstepping. The crane is assumed to be fixed and could not rotate, which is common for offshore cranes with very high capacity. The novelties of this work include: i) Modelling of the load dynamics in three degrees of freedom considering the impact from the vessel's DP. ii) Derivation of a reduced-order state-space model for control design that guarantees the stability of the full-order model. iii) Design of an underactuated nonlinear controller based on backstepping and command filtering approach for the reduced-order load model, taking into consideration the time-dependent DP controlled vessel position.

The rest of the paper is organized as the follows. Section II presents the problem definition and the physical modeling, Section III provides the control design, and Section IV shows the simulation results with a first principle crane vessel model, followed by the conclusions and recommendations.

2. PROBLEM FORMULATION

During offshore construction, the position of the heavy lift vessel is controlled by a DP system, while the force in the crane wires is controlled via a crane winch. For heavy lift vessels with hanging structures (i.e. loads), the proposed controller should be able to stabilize the position of the load in surge, sway, and heave position under DP control. In order to design the controller, we model the dynamics of the load under the impact of vessel DP.

When the load is free-hanging, the vessel and the load could be seen as connected by hoist wires. As the load's rotation has less impact on vessel's position stability compared to the impact from its position, the load dynamics can be described in 3 Degrees of Freedom (DoFs) as:

$$\begin{aligned}\ddot{\boldsymbol{p}}_{\mathrm{l}}^{\mathrm{n}}(t) =& -\boldsymbol{M}_{\mathrm{l}}^{-1}\boldsymbol{D}_{\mathrm{l}}\dot{\boldsymbol{p}}_{\mathrm{l}}^{\mathrm{n}}(t) - \boldsymbol{M}_{\mathrm{l}}^{-1}\boldsymbol{F}_{\mathrm{env}}(t) - \boldsymbol{M}_{\mathrm{l}}^{-1}\boldsymbol{g}_{\mathrm{l}} \\ &+ \frac{F_{\mathrm{hoist}}(t)}{||\boldsymbol{p}^{\mathrm{n}}(t) + \boldsymbol{R}^{T}(\boldsymbol{\Theta}(t))\boldsymbol{p}_{\mathrm{ct}}^{\mathrm{b}} - \boldsymbol{p}_{\mathrm{l}}^{\mathrm{n}}(t)||} \\ &\times \boldsymbol{M}_{\mathrm{l}}^{-1}(\boldsymbol{p}^{\mathrm{n}}(t) + \boldsymbol{R}^{T}(\boldsymbol{\Theta}(t))\boldsymbol{p}_{\mathrm{ct}}^{\mathrm{b}} - \boldsymbol{p}_{\mathrm{l}}^{\mathrm{n}}(t)), \end{aligned} \tag{1}$$

where $\boldsymbol{p}_{\mathrm{l}}^{\mathrm{n}}(t) \in \mathbb{R}^3$ is the position of the load, $F_{\mathrm{hoist}}(t)$ is the hoist force in the crane wires, $\boldsymbol{\Theta}(t) = [\phi, \theta, \psi]^T$ represents the rotation angles of the vessel, $\boldsymbol{p}^{\mathrm{n}}(t) = [x, y, z]^T$ is the position of the vessel in earth-fixed coordinate system, $\boldsymbol{R}^T(\boldsymbol{\Theta})$ is the rotation matrix from vessel's body-fixed coordinate system to the earth-fixed coordinate system. $\boldsymbol{F}_{\mathrm{env}}(t) \in \mathbb{R}^3$ is the environmental force. $\boldsymbol{M}_{\mathrm{l}} = m\boldsymbol{I}_{3\times 3}$ is the mass matrix of the load, with m denotes the mass of the payload and $\boldsymbol{I}$ denotes the identity matrix, $\boldsymbol{D}_{\mathrm{l}}$ is the damping matrix of the load. The last term in Eq. (1) represents the interconnected dynamics between the load position and the vessel movement, and $||\cdot||$ represents the Euclidean norm.

The control objective of this work is to define required hoist force in the crane wires (i.e. F_{hoist}), in order to keep the load in a desired position.

3. COMMAND FILTERED BACKSTEPPING CONTROL

In this section, a state space model is designed for the hanging load, and a control scheme is proposed based on backstepping and command filtering.

3.1 State-space modelling

Assuming no external disturbances, we can rewrite Eq. (1) in the following state space form:

$$\dot{\boldsymbol{\chi}}_1(t) = h(\boldsymbol{\Theta}(t)) - \boldsymbol{\chi}_2(t), \tag{2}$$

$$\dot{\boldsymbol{\chi}}_2(t) = f_0(\boldsymbol{\chi}_2(t)) + g_0(\boldsymbol{\chi}_1(t))u(t), \tag{3}$$

where $\boldsymbol{\chi}_1$ represent the vector of the crane wires (load to crane tip) in earth-fixed coordinate system, with the following representation:

$$\boldsymbol{\chi}_1(t) = \boldsymbol{p}^{\mathrm{n}}(t) - \boldsymbol{p}_{\mathrm{l}}^{\mathrm{n}}(t) + \boldsymbol{R}^{T}(\boldsymbol{\Theta}(t))\boldsymbol{p}_{\mathrm{ct}}^{\mathrm{b}}, \tag{4}$$

$$\boldsymbol{\chi}_2(t) = \dot{\boldsymbol{p}}_{\mathrm{l}}^{\mathrm{n}}(t), \tag{5}$$

$$\begin{aligned} h(t) &= \frac{d}{dt}(\boldsymbol{p}^{\mathrm{n}}(t) + \boldsymbol{R}^{T}(\boldsymbol{\Theta}(t))\boldsymbol{p}_{\mathrm{ct}}^{\mathrm{b}}) \\ &= \boldsymbol{R}^{T}(\boldsymbol{\Theta})\boldsymbol{v} + \frac{\partial}{\partial t}\boldsymbol{R}^{T}(\boldsymbol{\Theta})\boldsymbol{p}_{\mathrm{ct}}^{\mathrm{b}}) \end{aligned} \tag{6}$$

$$f_0(\boldsymbol{\chi}_2(t)) = -\boldsymbol{M}_{\mathrm{l}}^{-1}\boldsymbol{D}_{\mathrm{l}}\boldsymbol{\chi}_2(t) - \boldsymbol{M}_{\mathrm{l}}^{-1}\boldsymbol{g}_{\mathrm{l}}, \tag{7}$$

$$g_0(\boldsymbol{\chi}_1(t)) = \boldsymbol{M}_{\mathrm{l}}^{-1}\frac{\boldsymbol{\chi}_1(t)}{||\boldsymbol{\chi}_1(t)||}, \tag{8}$$

$$u(t) = F_{\mathrm{hoist}}(t), \tag{9}$$

where $\boldsymbol{v} \in \mathbb{R}^3$ denotes the velocity of the vessel, with

$$\boldsymbol{R}^{T}(\boldsymbol{\Theta}) = \begin{bmatrix} c_\psi c_\theta & -s_\psi c_\phi + c_\psi s_\theta s_\phi & s_\psi s_\phi + c_\psi c_\phi s_\theta \\ s_\psi c_\theta & c_\psi c_\phi + s_\phi s_\theta s_\psi & -c_\psi s_\phi - s_\theta s_\psi c_\phi \\ -s_\theta & c_\theta s_\phi & c_\theta c_\phi \end{bmatrix}, \tag{10}$$

where s_θ and c_θ are the sine and cosine of the angle θ (similarly for the remainder sines and cosines in (10)). Let us define

$$\frac{\partial}{\partial t}\boldsymbol{R}^T(\boldsymbol{\eta}) = \begin{bmatrix} R_{d11} & R_{d12} & R_{d13} \\ R_{d21} & R_{d22} & R_{d23} \\ R_{d31} & R_{d32} & R_{d33} \end{bmatrix}. \tag{11}$$

Then we have

$$R_{d11} = -c_\psi s_\theta \dot{\theta} - s_\psi c_\theta \dot{\psi}, \tag{12}$$

$$R_{d12} = (s_\psi s_\phi + c_\psi s_\theta c_\phi)\dot{\phi} + c_\psi c_\theta s_\phi \dot{\theta} + (-c_\psi c_\phi - s_\psi s_\theta s_\phi)\dot{\psi}, \tag{13}$$

$$R_{d13} = (s_\psi c_\phi - c_\psi s_\phi s_\theta)\dot{\phi} + c_\psi c_\phi c_\theta \dot{\theta} + (s_\phi c_\psi - s_\psi c_\phi s_\theta)\dot{\psi}, \tag{14}$$

$$R_{d21} = -s_\psi s_\theta \dot{\theta} + c_\psi c_\theta \dot{\psi}, \tag{15}$$

$$R_{d22} = (-c_\psi s_\phi + c_\phi s_\theta s_\psi)\dot{\phi} + s_\phi c_\theta s_\psi \dot{\theta} + (-s_\psi c_\phi + s_\phi s_\theta c_\psi)\dot{\psi}, \tag{16}$$

$$R_{d23} = (-c_\psi c_\phi + s_\theta s_\psi s_\phi)\dot{\phi} - c_\theta s_\psi c_\phi \dot{\theta} + (s_\psi s_\phi - s_\theta c_\psi c_\phi)\dot{\psi}, \tag{17}$$

$$R_{d31} = -c_\theta \dot{\theta}, \tag{18}$$

$$R_{d32} = c_\theta c_\phi \dot{\phi} - c_\theta s_\phi \dot{\theta}, \tag{19}$$

$$R_{d33} = -c_\theta s_\phi \dot{\phi} - s_\theta c_\phi \dot{\theta}, \tag{20}$$

The system described by Eq. (2) and Eq. (3) is an underactuated system which is not feedback linearizable, thus a reduced model with 2 DoFs is defined.

Let us define states ζ_1 and ζ_2,

$$\zeta_1(t) = ||\boldsymbol{\chi}_1(t)||, \tag{21}$$

$$\zeta_2(t) = -\frac{\boldsymbol{\chi}_1(t)^T \boldsymbol{\chi}_2(t)}{||\boldsymbol{\chi}_1(t)||}. \tag{22}$$

where $\zeta_1 > 0$ represents the time-varying length of the hoist wires.

The state space model becomes:

$$\dot{\zeta}_1(t) = \zeta_2(t) + f_1(\boldsymbol{\chi}_1(t), \boldsymbol{p}^n(t), \boldsymbol{\Theta}(t)), \tag{23}$$

$$\dot{\zeta}_2(t) = f_2(\boldsymbol{\chi}_1(t), \boldsymbol{\chi}_2(t)) - \frac{u(t)}{m}, \tag{24}$$

where

$$f_1 = \frac{\boldsymbol{\chi}_1^T}{||\boldsymbol{\chi}_1||} h, \tag{25}$$

$$f_2 = \frac{\boldsymbol{\chi}_1^T \boldsymbol{M}_1^{-1} \boldsymbol{D}_1 \boldsymbol{\chi}_2 + \boldsymbol{\chi}_1^T \boldsymbol{M}_1^{-1} \boldsymbol{g}_1}{||\boldsymbol{\chi}_1||} + (\frac{\boldsymbol{\chi}_2^T}{||\boldsymbol{\chi}_2||} - \frac{\boldsymbol{\chi}_1^T \boldsymbol{\chi}_2 \boldsymbol{\chi}_1^T}{||\boldsymbol{\chi}_1||^3})(h - \boldsymbol{\chi}_2). \tag{26, 27}$$

3.2 Backstepping control design

The backstepping control for the system (23)-(24) is based on the approach presented in (Farrell and Polycarpou, 2006). Suppose that Eq. (23) can be stabilized by a state feedback control law $\zeta_2 = \zeta_{2d}$; we define $\tilde{\zeta}_1 = \zeta_1 - \zeta_{1d}$, where

$$\zeta_{1d}(t) = ||\boldsymbol{\chi}_{1d}(t)|| = ||\boldsymbol{p}^{\mathrm{n}}(t) - \boldsymbol{p}_{ld}^{\mathrm{n}} + \boldsymbol{R}^T(\boldsymbol{\Theta}(t))\boldsymbol{p}_{\mathrm{ct}}^{\mathrm{b}}|| \tag{28}$$

is the desired signal for ζ_1. $\boldsymbol{\chi}_{1d}$ is the tracking signal for $\boldsymbol{\chi}_{1d}$, and $\boldsymbol{\eta}_{ld}$ is the desired position of the load. Initially, we find a control signal ζ_{2d} to solve the tracking control problem for the system

$$\dot{\zeta}_1 = \zeta_{2d} + f_1. \tag{29}$$

If we select

$$\zeta_{2d} = \dot{\zeta}_{1d} - k_1 \tilde{\zeta}_1 - f_1, \tag{30}$$

where $k_1 > 0$ is the control gain, then the controlled ζ_1 dynamics are

$$\dot{\tilde{\zeta}}_1 = -k_1 \tilde{\zeta}_1. \tag{31}$$

The time derivative of $V_1 = \frac{1}{2}\tilde{\zeta}_1^2$ satisfies

$$\dot{V}_1 = -\tilde{\zeta}_1 \dot{\tilde{\zeta}}_1 = -k_1 \tilde{\zeta}_1^2 \leq 0. \tag{32}$$

Consider now the second order system described by Eq. (23) and Eq. (24) and define $\tilde{\zeta}_2 = \zeta_2 - \zeta_{2d}$. Then the error dynamics are

$$\dot{\tilde{\zeta}}_1 = \zeta_{2d} + f_1 + \tilde{\zeta}_2 - \dot{\zeta}_{1d}, \quad \dot{\tilde{\zeta}}_2 = f_2 - \frac{u}{m} - \dot{\zeta}_{2d}, \tag{33}$$

where

$$\dot{\zeta}_{1d} = \frac{\partial}{\partial t}||\boldsymbol{\chi}_1|| = \frac{\partial ||\boldsymbol{\chi}_1||}{\partial \boldsymbol{\chi}_1}\dot{\boldsymbol{\chi}}_1 = \frac{\boldsymbol{\chi}_1^T \dot{\boldsymbol{\chi}}_1}{||\boldsymbol{\chi}_1||} = \frac{\boldsymbol{\chi}_1^T(\boldsymbol{R}^T(\boldsymbol{\Theta})\boldsymbol{p}^{\mathrm{n}} - \boldsymbol{v}_{\mathrm{l}} + \frac{\partial}{\partial t}\boldsymbol{R}^T(\boldsymbol{\Theta})\boldsymbol{p}_{\mathrm{ct}}^{\mathrm{b}})}{||\boldsymbol{\chi}_1||}, \tag{34}$$

with $\boldsymbol{v}_{\mathrm{l}} \in \mathbb{R}^3$ represents the velocity of the hanging load.

By applying Lemma 5.3.1 in (Farrell and Polycarpou, 2006), the control signal for the second order system will be

$$u_c = m(f_2 + k_2 \tilde{\zeta}_2 - \dot{\zeta}_{2d} + \tilde{\zeta}_1), \tag{35}$$

where $k_2 > 0$.

The Lyapunov function for the second order tracking error dynamics is $V_2 = V_1 + \frac{1}{2}\tilde{\zeta}_2^2$ that satisfies

$$\dot{V}_2 = \frac{\partial V_2}{\partial \tilde{\zeta}_1}\dot{\tilde{\zeta}}_1 + \frac{\partial V_2}{\partial \tilde{\zeta}_2}\dot{\tilde{\zeta}}_2 = \tilde{\zeta}_1 \dot{\tilde{\zeta}}_1 + \tilde{\zeta}_2 \dot{\tilde{\zeta}}_2 = \tilde{\zeta}_1(\zeta_{2d} + f_1 + \tilde{\zeta}_2 - \dot{\zeta}_{1d}) + \tilde{\zeta}_2(f_2 - \frac{u_c}{m} - \dot{\zeta}_{2d}) = -k_1\tilde{\zeta}_1^2 - k_2\tilde{\zeta}_2^2 \leq 0, \tag{36}$$

3.3 Command filtering

A command filter is designed to obtain ζ_{2d} and $\dot{\zeta}_{2d}$. First we consider the following structures

$$\zeta_{2d}^o = \dot{\zeta}_{1d} - k_1\tilde{\zeta}_1 - f_1 - \xi_2, \tag{37}$$

$$\dot{\xi}_1 = -k_1\xi_1 + (\zeta_{2d} - \zeta_{2d}^o), \tag{38}$$

$$u_c^o = -m(-k_2\tilde{\zeta}_2 + \dot{\zeta}_{2d} - f_2 - (\tilde{\zeta}_1 - \xi_1)), \tag{39}$$

$$\dot{\xi}_2 = -k_2\xi_2 - \frac{1}{m}(u_c - u_c^o), \tag{40}$$

where ξ_1 and ξ_2 are two bounded outputs of linear stable filters with bounded inputs, the command signal ζ_{2d}^o is filtered to obtain $\dot{\zeta}_{2d}$. With $\bar{\zeta}_i = \tilde{\zeta}_i - \xi_i, i = 1, 2$, we have

$$\begin{aligned}\dot{\tilde{\zeta}}_1 &= f_1 + \zeta_2 - \dot{\zeta}_{1d} \\ &= f_1 + \zeta_{2d}^o - \dot{\zeta}_{1d} + (\zeta_{2d} - \zeta_{2d}^o) + (\zeta_2 - \zeta_{2d}) \\ &= f_1 + (\dot{\zeta}_{1d} - k_1\tilde{\zeta}_1 - f_1 - \xi_2) - \dot{\zeta}_{1d} \\ &\quad + (\zeta_{2d} - \zeta_{2d}^o) + (\zeta_2 - \zeta_{2d}) \\ &= -k_1\tilde{\zeta}_1 + \bar{\zeta}_2 + (\zeta_{2d} - \zeta_{2d}^o), \end{aligned} \tag{41}$$

$$\begin{aligned}\dot{\tilde{\zeta}}_2 &= f_2 - \frac{1}{m}(u_c - u_c^o) - \frac{1}{m}u_c^o - \dot{\zeta}_{2d} \\ &= -k_2\tilde{\zeta}_2 - \frac{1}{m}(u_c - u_c^o) - \bar{\zeta}_1. \end{aligned} \tag{42}$$

Based on Eq. (38) to (42), we have

$$\dot{\bar{\zeta}}_1 = \dot{\tilde{\zeta}}_1 - \dot{\xi}_1 = -k_1\bar{\zeta}_1 + \bar{\zeta}_2, \tag{43}$$

$$\begin{aligned}\dot{\bar{\zeta}}_2 &= \dot{\tilde{\zeta}}_2 - \dot{\xi}_2 \\ &= -k_2\bar{\zeta}_2 - \bar{\zeta}_1. \end{aligned} \tag{44}$$

Consider the following Lyapunov function

$$V_3 = \frac{1}{2}\bar{\zeta}_1^2 + \frac{1}{2}\bar{\zeta}_2^2, \tag{45}$$

Then $\dot{V}_3 = -k_1\bar{\zeta}_1^2 - k_2\bar{\zeta}_2^2 \leq 0$. The origin of the $(\bar{\zeta}_1, \bar{\zeta}_2)$ is exponentially stable.

The filter is designed with the following structure:

$$\dot{\boldsymbol{\sigma}}(t) = \begin{bmatrix} 0 & 1 \\ -a_0 & -a_1 \end{bmatrix}\boldsymbol{\sigma}(t) + \begin{bmatrix} 0 \\ a_0 \end{bmatrix}\zeta_{2d}^o, \tag{46}$$

$$\begin{bmatrix} \zeta_{2d} \\ \dot{\zeta}_{2d} \end{bmatrix} = \boldsymbol{I}_{2\times 2}\boldsymbol{\sigma}(t), \tag{47}$$

with

$$s^2 + a_1 s + a_0 = 0 \tag{48}$$

is a stable Hurwitz polynomial.

Remark 1. In this paper, we assume that the position of the vessel $\boldsymbol{p}^n$, the rotation angle $\boldsymbol{\Theta}$, the position of the load $\boldsymbol{p}_{\mathrm{l}}^n$, and the hoist force F_{hoist} can be obtained by measurements. The terms $\dot{\phi}, \dot{\theta}, \dot{\psi}$ can be obtained from

$$\begin{bmatrix} \dot{\phi} \\ \dot{\theta} \\ \dot{\psi} \end{bmatrix} = \begin{bmatrix} 1 & s_\phi t_\theta & c_\phi t_\theta \\ 0 & c_\phi & -s_\phi \\ 0 & s_\phi/c_\theta & c_\phi/c_\theta \end{bmatrix} \begin{bmatrix} p \\ q \\ r \end{bmatrix}, \tag{49}$$

where p, q, and r represent the measurements of the angular rate of roll, pitch, and yaw of the vessel respectively.

Remark 2. The constant setpoint of the load position $\boldsymbol{p}_{\mathrm{ld}}^{\mathrm{n}}$ together with the DP system guarantee that the load is staying at the desired position. According to Eq. (28), Eq. (4) and Eq.(21), $\zeta_{1d}$is a function of $\boldsymbol{p}_{\mathrm{ld}}^{\mathrm{n}}$, $\boldsymbol{p}^{\mathrm{n}}(t)$, and $\boldsymbol{\Theta}(t)$, and is time-varying due to the changing of $\boldsymbol{p}^{\mathrm{n}}(t)$ and $\boldsymbol{\Theta}(t)$. This time-varying value of ζ_{1d} impacts on the load position generated from the movement of the vessel.

4. SIMULATION RESULTS

In this section, we present the simulation results of the application of the designed control scheme to system (1). The vessel position is controlled by a robust DP controller. The details of the vessel with DP system can be found in (Ye et al., 2019b). During the simulation, the load mass is set to 1000 tonnes. The desired load position is set to $[115, 0, -10]$. The control parameters are chosen as

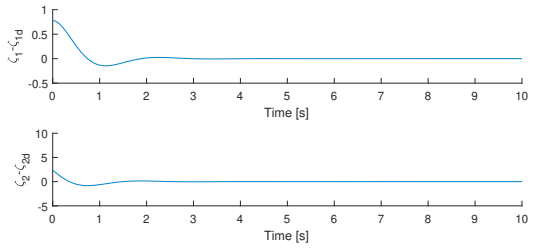

Fig. 2. $\tilde{\zeta}_1$ and $\tilde{\zeta}_2$ in first ten seconds with m=1000t

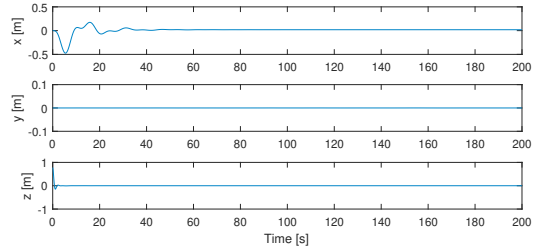

Fig. 3. $\boldsymbol{p}_{\mathrm{l}}^{\mathrm{n}} - \boldsymbol{p}_{\mathrm{ld}}^{\mathrm{n}}$ with m=1000t

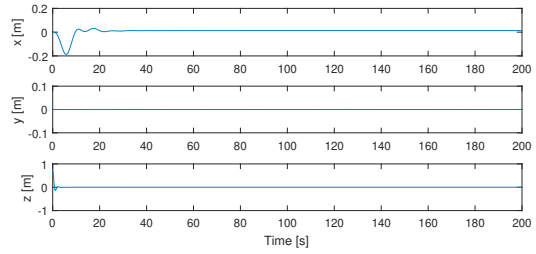

Fig. 4. $\boldsymbol{p}_{\mathrm{l}}^{\mathrm{n}} - \boldsymbol{p}_{\mathrm{ld}}^{\mathrm{n}}$ with m=500t

$$k_1 = 3, \tag{50}$$

$$k_2 = 3, \tag{51}$$

$$a_0 = 0.03, \tag{52}$$

$$a_1 = 0.2. \tag{53}$$

Simulation results are shown in Fig. 2 to Fig. 3. These figures show that the position of the load is stabilized with errors smaller than 1mm in x, y, and z direction with $\tilde{\zeta}_1$ and $\tilde{\zeta}_2$ approach zero gradually.

However, the high DoFs of the load model is simplified to a lower-DoF model. Thus the controlled position of the load might have small errors comparing to the desired position due to the reduced DoFs. This could be improved by further investigation of the setpoint of the heavy lift vessel's DP system.

Additional simulations are made to test the control system with a lower load (500 tonnes), and a higher load (2000 tonnes). Results are shown in Fig. 4. Simulations with different loads show that the performance of the controller improves as the load decreases. Fig. 6 shows the control input during the first five seconds of the three simulations. After five seconds, the control input is stable.

Simulation results in this section (i.e. Fig. 2 to Fig. 6) show that the position of the highly underactuated hanging load through the tension in the wires can be controlled

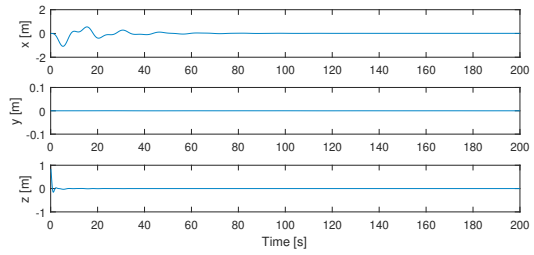

Fig. 5. $\boldsymbol{p}_{\mathrm{l}}^{\mathrm{n}} - \boldsymbol{p}_{ld}^{\mathrm{n}}$ with m=2000t

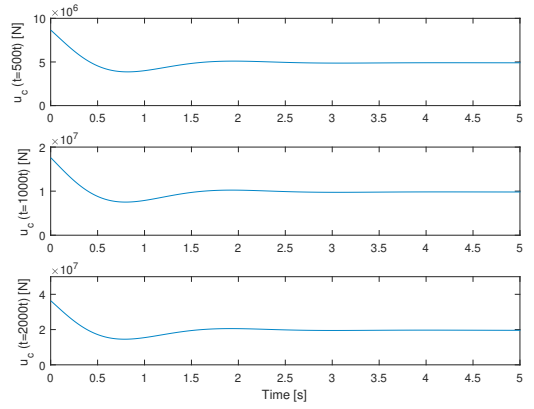

Fig. 6. Control Input of three simulations during first 5 seconds

and stabilized by applying backstepping and command filtering.

5. CONCLUSIONS AND FUTURE WORK

In this paper, we presented the design of a nonlinear control scheme for stabilizing the heavy load position during offshore operations of a crane vessel. The control design was based on the 3 DoFs dynamic model of the load motion, where the effects of the DP of the vessel were taken into account. Since the load system is underactuated, a reduced model was derived and a backstepping approach was followed for the design of the control. To avoid the differentiation of virtual control signals in the backstepping scheme, command filters were designed. Simulation results showed the effectiveness of the proposed control method to stabilize the load position. This enables the control and stabilization of hanging offshore load with large mass and with limited crane maneuverability, while the offshore heavy lift vessel is under DP control.

Future work will involve: i) The rigorous stability analysis taking into account environmental disturbances and sensor noise; ii) The optimization of the controller gains; iii) The interaction between the load controller and the DP controller.

REFERENCES

Chu, Y., Sanfilippo, F., Æsøy, V., and Zhang, H. (2014). An effective heave compensation and anti-sway control approach for offshore hydraulic crane operations. In *2014 IEEE International Conference on Mechatronics and Automation*, 1282–1287.

Fang, Y. and Wang, P. (2012). Advanced nonlinear control of an offshore boom crane. In *2012 American Control Conference (ACC)*, 5421–5426.

Fang, Y., Wang, P., Sun, N., and Zhang, Y. (2013). Dynamics analysis and nonlinear control of an offshore boom crane. *IEEE Transactions on Industrial Electronics*, 61(1), 414–427.

Farrell, J.A. and Polycarpou, M.M. (2006). *Adaptive approximation based control: unifying neural, fuzzy and traditional adaptive approximation approaches*, volume 48.

Harmsen, E., van Dijk, R., and Stuberg, P. (2018). Dp-stability during heavy lift operations using a modified kalman filter. In *ASME 2018 37th International Conference on Ocean, Offshore and Arctic Engineering*.

Hendrapati, M., Sumardi, J., Judhariksawan, Napang, M., Anshar, Subhandi, H., and Kristianto, Y. (2017). Offshore installation removal in the interest of navigation safety from international law point of view. *Journal of Law, Policy and Globalization*, 66, 194–204.

Ismail, R.R. and Ha, Q. (2013). Trajectory tracking and anti-sway control of three-dimensional offshore boom cranes using second-order sliding modes. In *2013 IEEE International Conference on Automation Science and Engineering (CASE)*, 996–1001.

Küchler, S., Mahl, T., Neupert, J., Schneider, K., and Sawodny, O. (2010). Active control for an offshore crane using prediction of the vessel's motion. *IEEE/ASME Transactions on Mechatronics*, 16(2), 297–309.

Li, R., Hansen, K., Beltrami, F., et al. (2016). A technical investigation on the ongoing evolution of the market of offshore installation vessels. In *SPE Annual Technical Conference and Exhibition*.

Lu, B., Fang, Y., and Sun, N. (2019). Nonlinear coordination control of offshore boom cranes with bounded control inputs. *International Journal of Robust and Nonlinear Control*, 29(4), 1165–1181.

Lu, B., Fang, Y., Sun, N., and Wang, X. (2017). Antiswing control of offshore boom cranes with ship roll disturbances. *IEEE Transactions on Control Systems Technology*, 26(2), 740–747.

Messineo, S. and Serrani, A. (2009). Offshore crane control based on adaptive external models. *Automatica*, 45(11), 2546–2556.

Nam, B., Hong, S., Kim, Y., Kim, J., et al. (2013). Integrated simulations of a floating crane installation vessel with dp systems in waves. In *The Twenty-third International Offshore and Polar Engineering Conference*.

Ngo, Q.H., Nguyen, N.P., Nguyen, C.N., Tran, T.H., and Bui, V.H. (2019). Payload pendulation and position control systems for an offshore container crane with adaptive-gain sliding mode control. *Asian Journal of Control*.

Nguyen, N.P., Ngo, Q.H., and Ha, Q.P. (2015). Active control of an offshore container crane. In *2015 15th International Conference on Control, Automation and Systems (ICCAS)*, 773–778.

Qian, Y., Fang, Y., and Lu, B. (2017). Adaptive repetitive learning control for an offshore boom crane. *Automatica*, 82, 21 – 28.

Sun, X., Huang, D., and Wu, G. (2012). The current state of offshore wind energy technology development. *Energy*, 41(1), 298–312.

Sun, Y.G., Qiang, H.Y., Xu, J., and Dong, D.S. (2017). The nonlinear dynamics and anti-sway tracking control for offshore container crane on a mobile harbor. *J. Marine Sci. Technol.-Taiwan*, 25(6), 656–665.

Ye, J. (2016). Dynamic positioning during heavy lift operations: Using fuzzy control techniques, nonlinear observer and h-infinity method separately to obtain stable dp systems for heavy lift operations.

Ye, J., Godjevac, M., Baldi, S., and Hopman, H. (2019a). Joint estimation of vessel position and mooring stiffness during offshore crane operations. *Automation in Construction*, 101, 218–226.

Ye, J., Godjevac, M., and el Amam, E. (2017). Position control of crane vessel during offshore installations: Using adaptive and robust control methods. In *2017 21st International Conference on System Theory, Control and Computing (ICSTCC)*, 17–22.

Ye, J., Roy, S., Godjevac, M., and Baldi, S. (2019b). Observer-based robust control for dynamic positioning of large-scale heavy lift vessels. *IFAC-PapersOnLine*, 52(3), 138–143.